



---

## **MECHANICAL MODEL OF A TERRAPOWER, TRAVELING WAVE REACTOR FUEL ASSEMBLY DUCT**

**Michael Cohen<sup>1</sup>, Mark Werner<sup>2</sup>, and Chris Johns<sup>3</sup>**

<sup>1</sup> Mechanical Analyst, TerraPower, LLC, Bellevue, WA

<sup>2</sup> Mechanical Methods and Development Engineer, TerraPower, LLC, Bellevue, WA

<sup>3</sup> Nuclear Scientist/Engineer, TerraPower, LLC, Bellevue, WA

### **ABSTRACT**

The concept of a breed-and-burn reactor was envisioned many years ago as a potential alternative to the traditional breeder reactor design which relies on reprocessing of the nuclear fuel. However, limitations on both computational capabilities and fuel assembly structural materials prevented significant development of this concept until recently. This paper describes the mechanical computational models used by TerraPower, LLC to predict bowing behavior of fuel assembly ducts in a Traveling Wave Reactor (TWR).

In the development of these analytical tools, TerraPower has developed benchmark models for comparison with published results for metal fast reactor designs, such as found in the work by Kalinowski (1981). Specifically, this analysis focuses on the bowing behavior of a single fuel assembly duct under temperature and fast flux gradients.

The integration of these improved reactor core mechanical computational capabilities with analytical tools representing other disciplines contributes greatly to the development of the TerraPower Traveling Wave Reactor.

### **INTRODUCTION**

The concept of a breed-and-burn reactor was envisioned many years ago as a potential alternative to the traditional breeder reactor design which relies on reprocessing of the nuclear fuel (Feinberg, 1958). However, limitations on both computational capabilities and fuel assembly structural materials prevented significant development of this concept until recently. A Traveling Wave Reactor (TWR) is a class of liquid metal reactor (LMR) that is uniquely designed to operate after startup using only natural or depleted uranium. The waves that breed and deeply burn fissile nuclides in-situ travel relative to the fuel and provide the possibility for very long core life. This long core life allows for significantly higher fuel utilization than light water reactors (LWRs) (Hejzlar et al., 2013).

TerraPower, LLC, has developed significantly improved analysis tools that integrate multiple engineering disciplines including neutronics, thermal hydraulics, safety, and structural mechanics (Touran et al., 2012). This paper describes the subset of structural mechanics computational tools in terms of their scope, capabilities, and a comparison with published results. The comparison with published data gives the engineer an understanding of system behavior under specified conditions. With this understanding, the engineer can utilize available high performance computing, exploit state-of-the-art modeling capabilities, and integrate with other software codes to explore optimized and innovative solutions to the TWR design challenges at hand.

### **FAST REACTOR DESIGN CHALLENGES**

Significant literature is available on the United States' Department of Energy (DOE) liquid metal reactor (LMR) designs. This includes the Experimental Breeder Reactor II (EBR-II) (Shields, 1981), the Fast Flux Test Facility (FFTF) (Hecht, 1981), and the Clinch River Breeder Reactor Project (CRBRP)

(Kalinowski and Swenson 1974)). Although the CRBRP was not constructed, the design and engineering work that went into it was based on knowledge gained during the design, construction, and operation of EBR-II and FFTF. The CRBRP core design serves as the basis for the design of a modern, large scale limited free bow core. Thus, core mechanical models developed for use of the TWR may be compared to CRBRP published data to understand its behavior.

LMR designs face common structural challenges in the design of their core and their core components. These challenges result from the high fluence and high temperatures found in an LMR.

### ***Duct Dilatation and Bowing***

The high temperatures and fluence found in the LMR fuel pin cladding cause thermal creep and void swelling of the cladding material. The fuel pin assemblies are closely packed within a hexagonal duct (also referred to as wrapper). The duct provides a boundary for internal flow of coolant. It also provides a load path for lifting and handling of the fuel assembly.

Similar to the fuel pin cladding, the duct is susceptible to void swelling. Duct temperatures are not as high as cladding temperatures; and do not result in significant thermal creep. However, the pressure differential between the internal duct flow and the interstitial sodium filled space between the ducts results in a net internal pressure on the duct walls. This causes stresses, which, in turn, cause irradiation creep. The radial distortion in the duct resulting from the combination of irradiation creep and void swelling is referred to as duct dilatation.

Radially, the temperature and the fast flux profile in the reactor core are not uniform. Both duct wall temperature and fast flux tend to be higher towards the center and decrease in the radially outward direction. An example of the radial temperature and fast flux profiles from the CRBRP is shown in Figure 11 and Figure 12 of Kalinowski and Swenson (1974). At beginning of life, the steepest gradients occur at the fuel-radial blanket interface. At end of life, gradients are steepest in fuel assemblies adjacent to the control assemblies (Kalinowski, 1981).

Axially, the temperatures in the duct wall increase from the inlet temperature in the active fuel region of the fuel assembly. The temperature quickly approaches the duct outlet temperature just above the active fuel region. The axial distribution of fast flux is centered and peaks at the center of the active fuel region. It decreases below and above this region depending on the fuel composition in the core. A single fuel assembly will have temperature and fluence gradients across opposing faces. Typical axial profiles for the CRBRP from Figures 11 and 12 of Kalinowski and Swenson (1974) are reproduced on Figures 1 and 2. The differential thermal expansion and differential void swelling resulting from the gradients causes assembly bow. The bowing changes over time as loads change and the fuel assemblies interact. This behavior is described by Kalinowski and Swenson (1974), Shields (1980), Kamal and Orechwa (1986). It is summarized in Table 1 and pictorially represented in Figure 3.

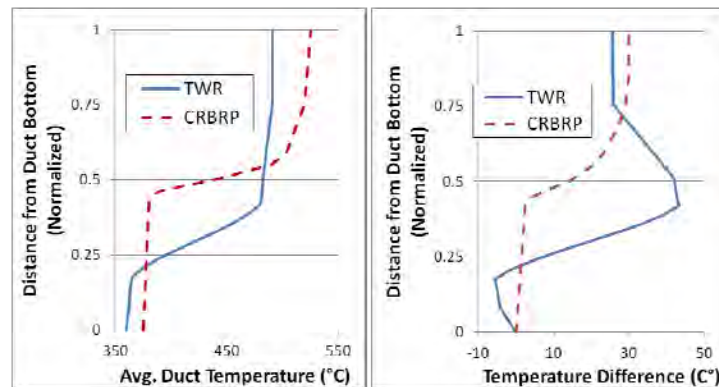


Figure 1. Duct Wall Average Axial Temperature Distribution and the Duct Flat-to-Flat Temperature Gradient (Shown as Temperature Difference between Duct Faces) at a Distance from the Duct Bottom

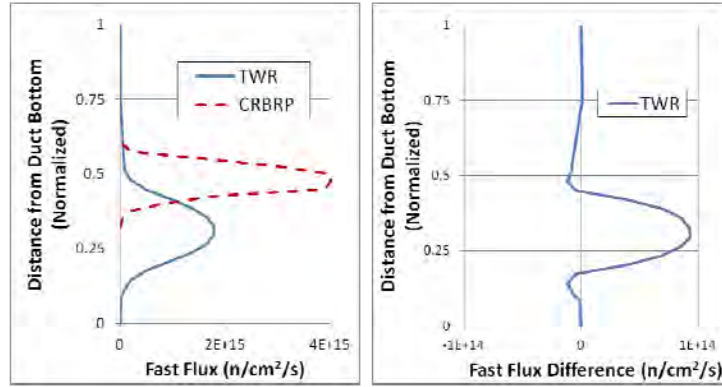


Figure 2. Duct Wall Average Fast Flux and the Duct Flat-to-Flat Flux Gradient (Shown as Flux Difference between Duct Faces) at a Distance from the Duct Bottom

Table 1: Description of Shapes That May be Found in a Bowed Duct

1	At start up, a duct bows because of temperature gradients: the hotter faces grow more in length than the cooler faces. Bowing is in the direction of the lower temperature face (sketch (1)).
2	Ducts continue to bow until the load pads contact adjacent fuel assembly load pads. These constraints introduce an S-shape in the duct (2).
3	Unconstrained bowing shape after irradiation creep at the core refueling temperature.
4	Unconstrained bowing shape after irradiation creep and void swelling at the core refueling temperature. If swelling were to dominate irradiation creep, the duct would appear as in sketch (4a). Most likely, the irradiation creep and swelling offset each other (Boltax, 1978 and Shields, 1980) as shown in sketch (4b).

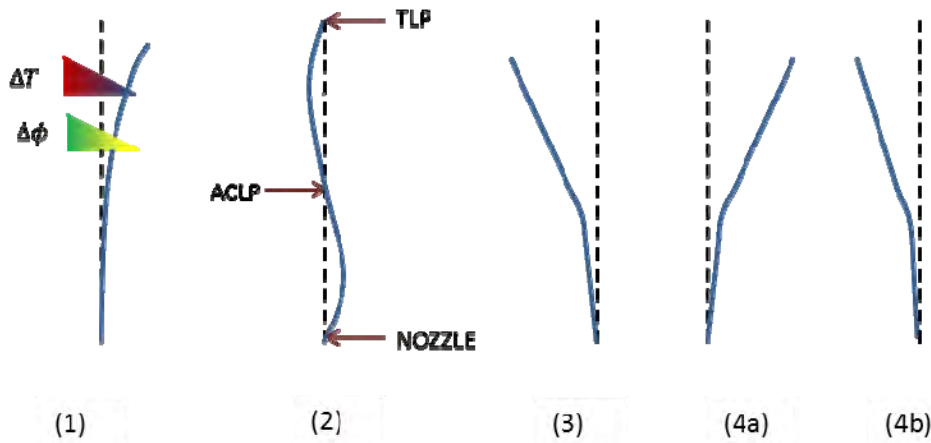


Figure 3. Schematic Views of Bowed Duct Shapes (Kalinowski, 1974).

### ***Core Restraint System***

The system of fuel assemblies, other core components such as shield assemblies, and the supporting structure is commonly referred to as the core restraint system. The bowing and interaction of fuel assembly ducts has several implications with respect to the performance and management of the LMR core. Kalinowski (1974) identified the performance requirements of a core restraint system as summarized in Table 2.

Table 2: Core Restraint System Performance Requirements

Requirement		Concern
1	Reactivity control	Expansion and bowing affect the reactivity in the core. As the bowed shapes change during power-up or a transient condition, the reactivity of the reactor may change too.
2	Core management	Excessive bowing could make fuel assemblies difficult to locate for interfacing equipment if the handling socket moves to a location too far from its nominal position.
		As assemblies bow and distort, they may become more difficult to withdraw or reinsert into the core as the handling equipment must overcome contact forces and interferences.

The two performance requirements compete with each other. In order to have good reactivity control, small interassembly and core former gaps are desirable so that duct bowing is predictable. However, larger interassembly gaps help to minimize withdrawal and insertion loads.

Because of irradiation creep and void swelling, the core restraint system's behavior changes over time. As assemblies bow and come into contact, they apply forces to each other and the surrounding restraint ring (or core former). These forces induce irradiation creep and may oppose forces from constrained swelling.

At refueling, the residual lateral forces resulting from the reversing of the temperature loads determine the frictional forces at which assemblies may be withdrawn or inserted into the core. As stated by Pennell (1975), the design must consider irradiation creep, swelling, and their superposition.

### **TWR DESIGN CHALLENGES**

The TWR has the same design challenges as described above, but to a greater extent. "High fuel burnup necessary to achieve a breed-and-burn operating model with depleted uranium feed fuel requires long residence time in-core and therefore high fast neutron fluence" (Hejzlar et al., 2013). Although this long residence time has many advantages with respect to power production and fuel utilization, assemblies accumulate significantly higher fluence than assemblies in typical fast reactors. This higher fluence results in a higher structural performance requirement in materials that make up the structure of the removable core components.

Although the high dose reached to date in metal fueled test pins made from low-swelling HT-9 cladding is ~200 displacements per atom (DPA), the TWR peak dose in the cladding may reach ~500-600 DPA (Hejzlar et al., 2013). Thus, the TWR ducts and core restraint system will need to accommodate the high accumulated fluences in the duct material, high temperatures, and pressure loads.

A first step in being able to address these challenges is to use the material models developed by TerraPower for the TWR to look for similar behavior in the fuel assembly ducts as was predicted in the CRBRP and observed in EBR-II and FFTF.

## **SINGLE FUEL ASSEMBLY MODEL**

Given the complexity and computational cost of modeling an entire core section, preliminary models focus on a single fuel assembly duct constructed of the ferritic-martensitic steel, HT-9. This approach allows the engineer the opportunity to understand and predict duct distortion in a somewhat simplified manner. In order to understand the bowing behavior of this assembly, the duct is modeled as residing in one of the largest temperature gradient and largest fast flux gradient regions in the core. As was discussed earlier, this can be on the outer ring of fuel assemblies, adjacent to blanket assemblies, or in a fuel assembly adjacent to a control assembly.

The TerraPower neutronics and thermal hydraulics codes generate output for the entire core that provide direct input into the single duct model. These parameters include fast flux and duct temperature, and net internal pressure. The fast flux and duct wall temperature vary through the cross section of the duct. Plots of duct wall temperatures are shown in Figures 1 and 2. In comparison to the CRBRP distributions, the TWR average axial temperatures are similar in the curve shape, but have different inlet and outlet conditions. Also, the temperatures are shifted axially due to different fuel compositions in the axial directions. The temperature gradients differ significantly. Most notably, the TWR temperature gradient is less significant above the active core region in comparison to the CRBRP temperature gradient. The fast flux distribution also has a similar shape, and differs due to fuel composition and neutronic performance.

A single assembly model is constructed using either commercial finite element code ANSYS or ABAQUS along with custom material behavior routines. The use of these commercial codes allows for various enhancements at low cost that were not achievable with simple beam and gap element models.

The duct is pinned at its base and interaction with adjacent core components is modeled at the axial locations of the above core load pad (ACLP) and top load pad (TLP).

The loads are applied over each defined burn cycle. After each burn cycle, the flux load is removed and the assembly is isothermally cooled to the refueling temperature. In order to see the net shape of the assembly at the end of its last irradiation cycle, the boundary conditions at the ACLP and TLP are removed in one final load step.

### ***Bowing Shapes***

Initially, a series of simple models are run to see how the TWR material model behaves in comparison to reference data. The first model has a temperature gradient only and is not constrained at the ACLP or TLP. In essence, it acts as a “free bow” assembly. Figure 4(a) shows that the assembly bows in the expected direction.

The second model is also not irradiated and is also under temperature gradient loads only. However, it is constrained at the ACLP and TLP. Figure 4(b) shows that the shape is not the expected S-shape: the duct bows inward both above and below the ACLP. Modifying the temperature gradient so that it more closely matches the CRBRP axial temperature distribution affects the bowing shape. The inward bowing in the active core region nearly disappears and the duct more closely resembles the S-shape as reported by Kalinowski and Swenson (1974). This is shown in Figure 4(c).

Looking at the temperature profiles in Figure 1, we see that the TWR average temperature increases at a lower axial position when compared to the CRBRP case. Similarly, the TWR temperature gradient is largest at a much lower axial position and extends both above and below the ACLP. The TWR temperature gradient peaks in the active fuel region and diminishes in the upper duct. In comparison, the CRBRP temperature gradient increases near the ACLP and becomes constant in the upper duct. With the TWR temperatures, the bowing shape is driven by the temperature gradient which is both below and

above the ACLP. The duct wants to elongate on the “high” side of the gradient. By shifting the temperatures and gradient higher with respect to the ACLP, the upper duct now drives the bowing shape. Lastly, the relative location of the ACLP in the duct affects the bowing shape. Even with the CRBRP-like temperature profile, the duct does not bow in an ideal S-shape.

Also note that a ferritic-martensitic stainless steel such as HT-9 has an instantaneous coefficient of linear thermal expansion of  $13.1 \times 10^{-6}$  mm/mm/°C at 500°C (ASME, 2007). The value for austenitic stainless steel at the same temperature is  $20.2 \times 10^{-6}$  mm/mm/°C. Thus, for the same duct length and the same temperature distributions, a duct constructed of HT-9 will grow less thermally than a duct constructed of an austenitic stainless steel. The HT-9 duct will also have a smaller difference in longitudinal growth between its hot and cold faces. The result is that the HT-9 duct bows less than an austenitic duct.

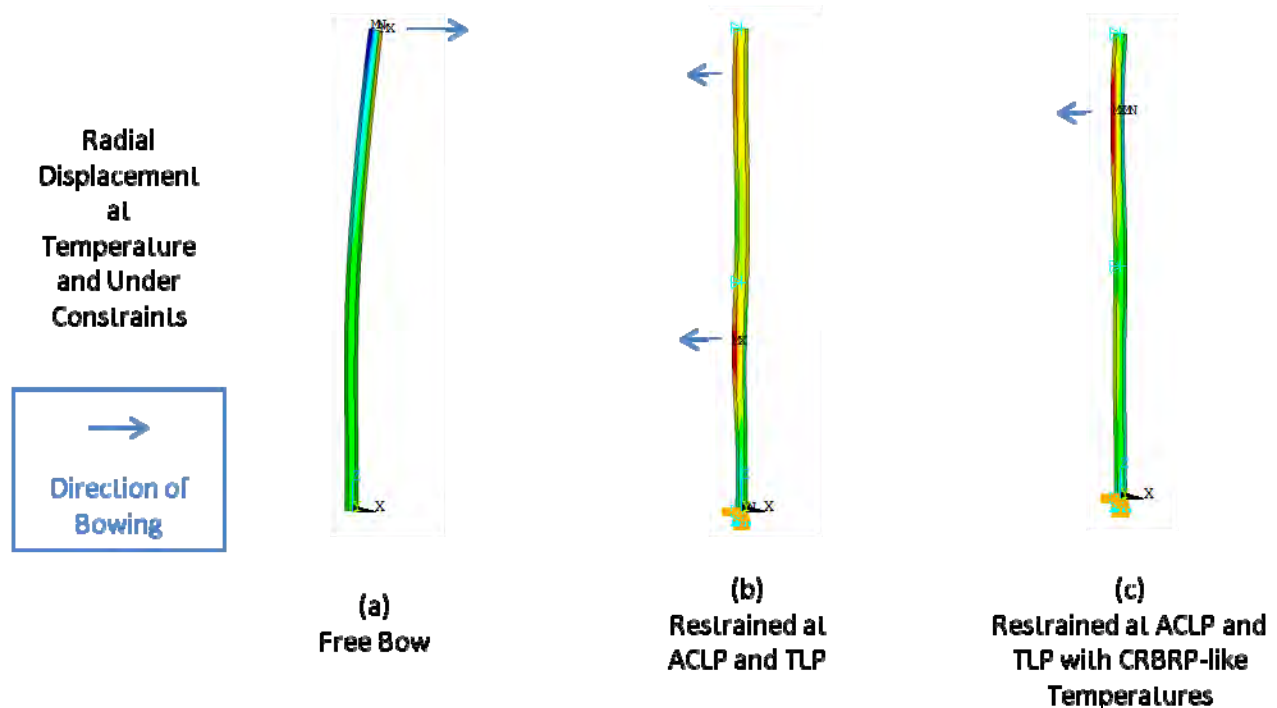


Figure 4. Unirradiated Bow due to Thermal Gradients

Figure 5(a) shows results for a model where irradiation creep is active in the material model. The first contour plot shows the shape after irradiation, but prior to cooling. The second contour plot is at the refueling temperature, and the ACLP and TLP boundary conditions have been removed in the model. This final shape shows that the initial stresses reduced over time due to irradiation creep. Upon cooling, the temperature loads reverse, and the duct bows past its initial position.

The void swelling model (Figure 5(b)) shows that the bowing occurs in the same direction as the thermal bowing. Unlike the elastic thermal free bow model, the void swelling is inelastic leaving the net deformed shape.

Figure 5(c) shows the final shape for the duct that can undergo both irradiation creep and void swelling. The net shape shows that the irradiation creep and void swelling oppose each other. In this case, the final shape is in the reversed direction. However, it should be noted that the final shape is sensitive to material irradiation creep and swelling rates, the state of stress in the duct, temperature profiles, duct geometry and ACLP location.

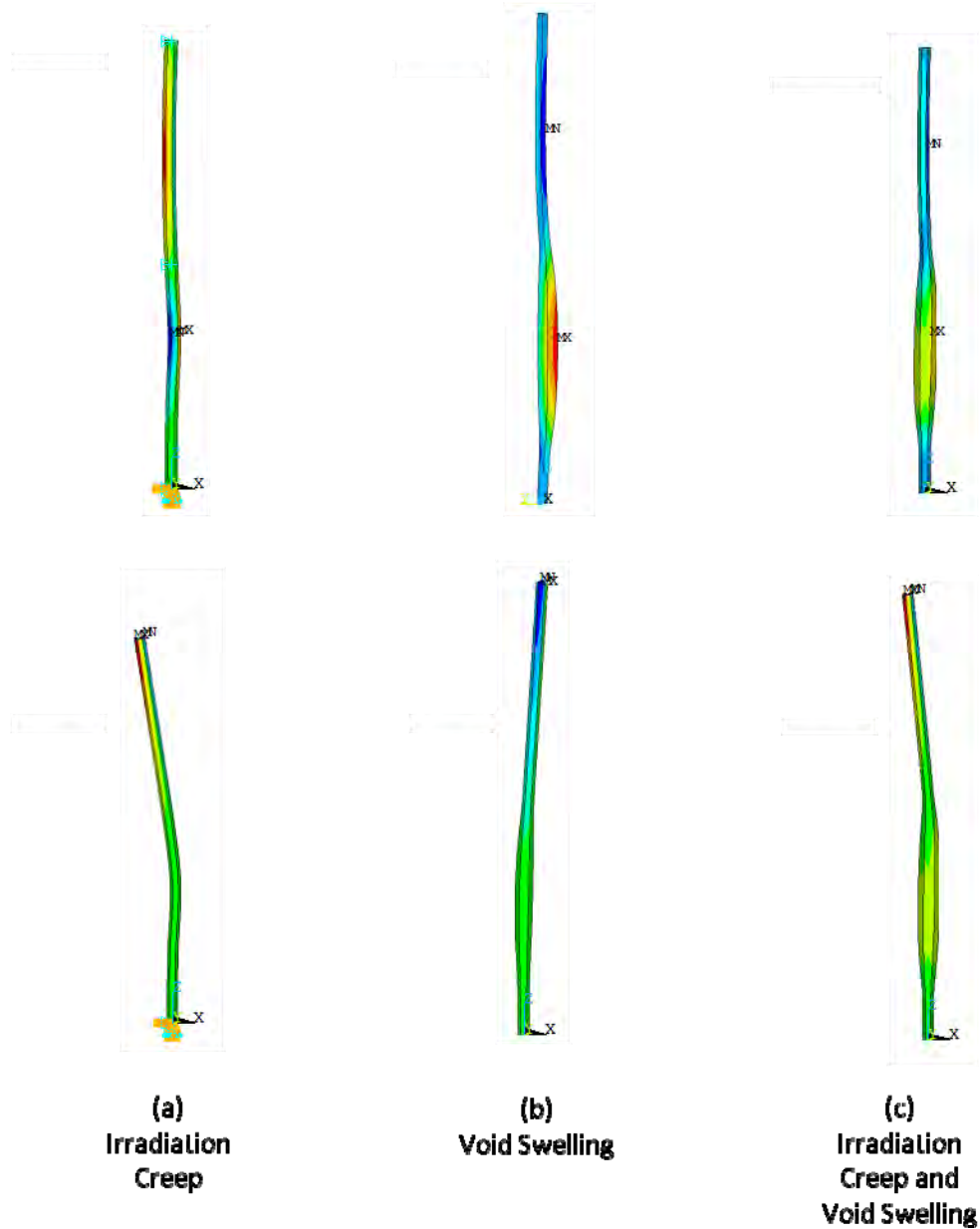


Figure 5. Inelastic Bowing and Residual Deformations at Refueling Conditions

Figure 6, shows the bowed duct that has undergone irradiation creep and swelling for an illustrative 25 cycles. The model ignores contact that may occur with adjacent core components in the active core region. The associated plot shows the relative radial deflection in the active core region and in the region between the ACLP and the TLP. In the active fuel region, the duct wall initially distorts radially at a high rate. The creep then levels off. However, once the void swelling incubation period has been reached, the dilation due to swelling continues to grow. Above the ACLP, the bowing displacement also creeps initially at a high rate, but it levels off and quickly: The increase in creep strain changes (and reduces) the state of stress; thereby, limiting further creep strain.

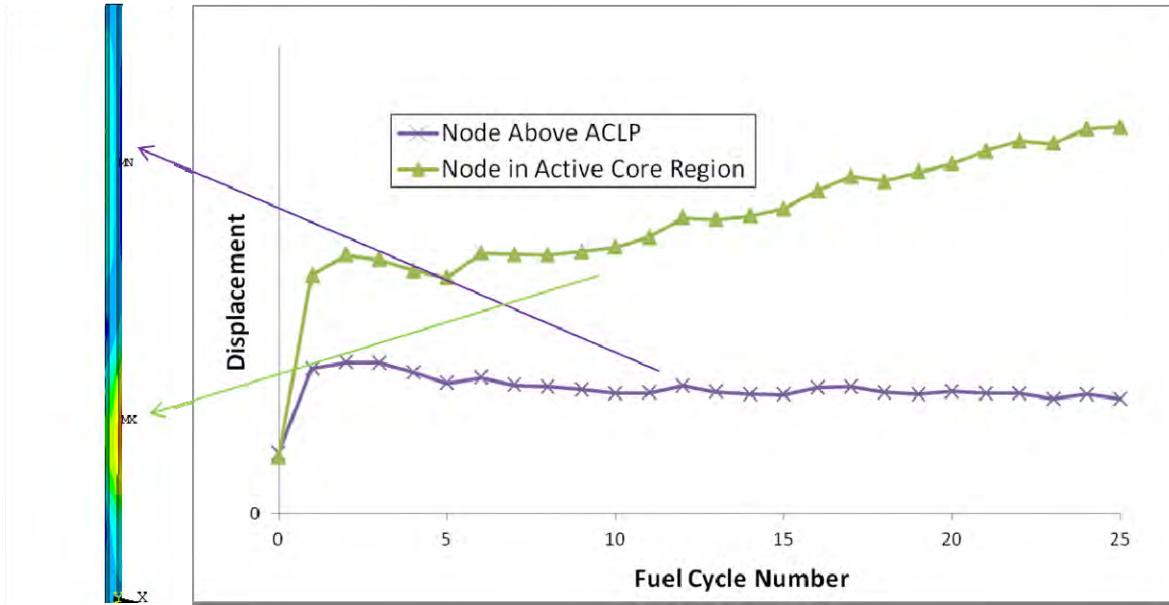


Figure 6. Comparison of Center-to-Flat Distortion in Active Core Region vs. Above the ACLP

### ***Bowing Forces***

Figure 7 shows the contact forces at the end of each fuel cycles at the nozzle, ACLP, and TLP locations. They are based on the contact forces at the three locations once the fast flux load is removed and the temperature reaches the refueling temperature. Similar to Figure 9 in Kalinowski (1981), the inter-assembly contact force is non-zero after the first fuel cycle, e.g. 2300N for the ACLP. This non-zero force exists because irradiation creep reduces the inter-assembly contact forces during irradiation. When the loads are reversed and the fast flux is removed, the reaction forces reverse elastically. This leaves a residual contact force plotted for the first set of points on the graph.

At the end of the second cycle, the contact forces increase (from 2300N to 2750N at the ACLP), but the increase is not as much as after the first cycle. Figure 8 illustrates this behavior using the TLP contact force in the x-direction as an example. The initial -1200N contact force diminishes asymptotically towards zero over time. At the end of each fuel cycle, the change in contact force is constant and is equal in magnitude and opposite in direction to the initial contact force. For the TLP in the x-direction, the refueling contact force is equal to the end of cycle contact force plus 1200N. As the end of cycle contact force levels off, the change to the refueling contact force becomes less significant.

After the fourth load cycle, it is apparent that the void swelling incubation is complete. There is a noticeable, but small, increase in the reaction forces. Stresses introduced by restrained void swelling are mitigated by irradiation creep. This behavior shows that HT-9 ducts and the limited free bow core restraint can be used to offset forces resulting from void swelling. This has the effect of minimizing the required assembly and core former gaps (yielding predictable behavior with respect to reactivity changes due to bowing) and aiding core management (by minimizing the increase in contact and retrieval forces).

Unlike Kalinowski's similar plot (Figure 9, 1981), the TLP contact force loads do not continue to grow over subsequent fuel cycles. The material models, geometry, and loads between the CRBRP and the TWR differ enough such that in the TWR case, the void swelling is limited at the ACLP and the TLP by irradiation creep.

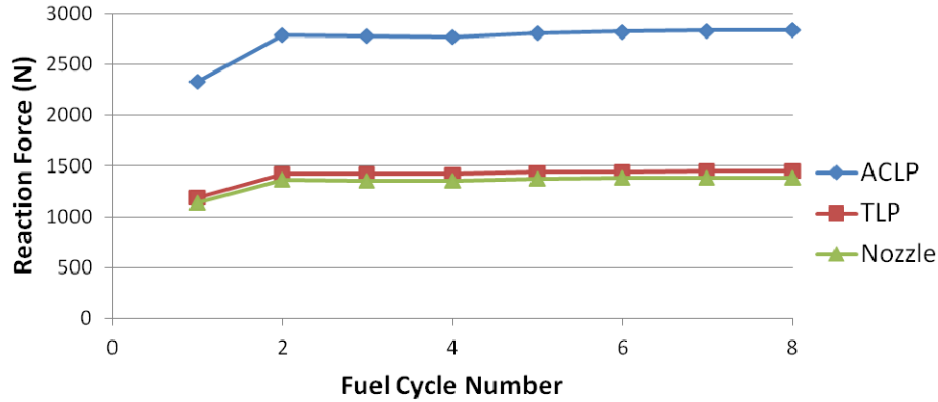


Figure 7. Total Lateral Loads at the End of Each Cycle

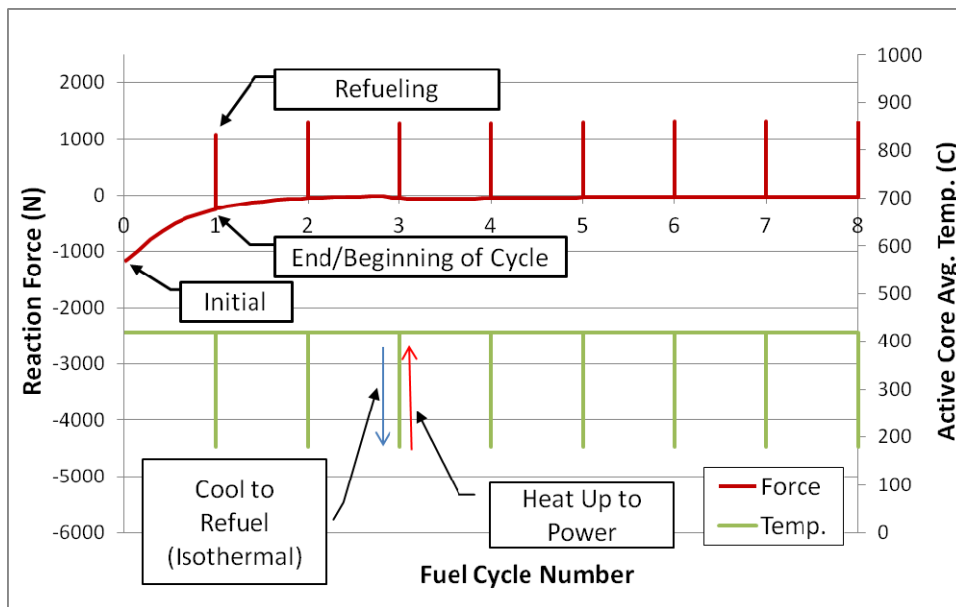


Figure 8. Top Load Pad (TLP) Reaction Forces in the x-direction

## CONCLUSION

The pursuit of a viable TWR design has driven TerraPower to develop custom material performance models in conjunction with commercially available finite element analysis software to understand the challenges of a very high burnup and long life core design. Three dimensional FEA models of a single fuel assembly duct show that bowing behavior is comparable to predictions made for the CRBRP. As with the CRBRP and other LMR designs, we see that irradiation creep is self-limiting, but void swelling needs to be controlled. It is desirable to use low void swelling materials which can limit the inter-assembly forces generated in a limited free bow core. Differences in predicted behavior are attributable to fuel design specific gradients in the respective core concepts, material properties and duct geometry.

The single assembly model and future finite element models can be used to design the ducts and ensure that the core restraint system can satisfy its basic performance requirements: reactivity control and core management. With these fundamental understandings of core behavior, design solutions may be explored to further optimize the TWR design.

## REFERENCES

- ASME (2007). *ASME Boiler and Pressure Vessel Code, Section II-Materials, Part D – Properties (Metric)*, 2007, New York, NY, USA.
- Boltax, et al., (1978). “Design Applications of Irradiation Creep and Swelling Data”, *ANS Meeting*, San Diego, CA, June 1978.
- Feinberg S. M. (1958). “Discussion Comment,” *Rec. of Proc. Session B-10*, ICP UAE, No. 2, Vol. 9, p. 447, United Nations, Geneva, Switzerland.
- Fox, J. N. (1979). “Influence of Core-Assembly Refueling Requirements on LMFBR Core-System Design,” *Third U.S. National Congress on Pressure Vessels and Piping*, San Francisco, CA, June 25-29, 1979, GEF-SP-146.
- Hejzlar, Pavel, et al., (2013). “TerraPower, LLC Traveling Wave Reactor Development Program Overview,” *Proceedings of ICAPP 2013, Paper No. FA226*.
- Hecht, S. L. (1981). “FFTF Core Component Duct Lifetime: Criteria and Core Management Methods,” *Joint Conference of the Pressure Vessels and Piping, Materials, Nuclear Engineering and Solar Divisions (ASME)*, Denver, CO, June 21-25, 1981.
- Kalinowski, J. E. (1981). “The Effect of Irradiation Induced Structural Material, Deformations on Core Restraint Design,” Westinghouse, Advanced Reactors Division, Madison, PA, USA, CONF-810625-21.
- Kalinowski, J. E., and Swenson, D. V. (1974). “Nonlinear Analysis of the CRBR Core Restraint System,” Westinghouse, Advanced Reactors Division, Waltz Mill, PA, USA, CONF-760451-3.
- Kamal, S. A. and Orehwa, Y. (1986). “Transient Bowing of Core Assemblies in Advanced Liquid Metal Fast Reactors,” *Advances in Reactor Physics and Safety Meeting*, Saratoga Springs, NY, USA, 17 Sep 1986.
- Moran, T. J. (1988). “Core Restraint Design for Inherent Safety,” *Nuclear Power Conference*, Myrtle Beach, SC, April 17-20, 1988.
- Pennell, W. E. (1975). “CRBR Reactor Structures Design,” *Proceedings of the Breeder Reactor Corporation*, Los Angeles, CA, April 16, 1975.
- Shields, J. A., (1981). “Bow in Experimental Breeder Reactor II Reflector Subassemblies,” *Nuclear Technology*, Vol. 52, pp. 214-227.
- Sutherland, W. H., (1984). “Overview of Core Designs and Requirements/Criteria for Core Restraint Systems,” *IAEA IWGFR Specialists Meeting, Mottram Hall*, South Manchester, England, October 1-4, 1984.
- Touran, N., Cheatham, J. and Petroski, R. (2012). “Model Biases in High-Burnup Fast Reactor Simulations”, *Advances in Reactor Physics – Linking Research Industry and Education*, PHYSOR 2012, Knoxville, Tennessee, USA.